

## The sampling-based dynamic procedure as tool for higher-order discretization

D. Fauconnier<sup>\*,†</sup>, C. De Langhe and E. Dick

*Department of Flow, Heat and Combustion Mechanics, Ghent University, St.-Pietersnieuwstraat 41,  
9000 Gent, Belgium*

### SUMMARY

Accuracy improvement is demonstrated by alternative use of a recently proposed LES formalism based on sampling operators. It is shown that the sampling-based dynamic procedure, in combination with an appropriate truncation error model, can be used as a technique to increase the numerical accuracy of a discretization. The technique is resemblant to Richardson extrapolation. The procedure is tested on a 2D lid-driven cavity at  $Re=400$  using a finite difference method. Promising results are obtained. Copyright © 2007 John Wiley & Sons, Ltd.

Received 23 March 2007; Revised 25 September 2007; Accepted 27 September 2007

KEY WORDS: dynamic procedure; high-order accuracy; Richardson extrapolation

### 1. INTRODUCTION

A *sampling formalism* for large eddy simulation (LES) was proposed by Winckelmans *et al.* [1] and Knaepen *et al.* [2], which is a projection method for Navier–Stokes equations from continuum space to a discrete space using a sampling operator instead of a filter operator. Since the sampling operator does not commute with spatial derivatives, a closure term appears which represents the loss of information due to the projection on the discrete mesh. In [1, 2] a Smagorinsky model was proposed that, by relying on a generalized dynamic procedure, succeeded in accounting for the subgrid scales. The technique is meant to model turbulent subgrid stresses, but as it fundamentally describes the projection error on a discrete mesh, it might as well be used to model the truncation error of the discretization. In previous work, we investigated the ability of this *sampling-based*

---

\*Correspondence to: Dieter Fauconnier, Department of Flow, Heat and Combustion Mechanics, Ghent University, St.-Pietersnieuwstraat 41, 9000 Gent, Belgium.

†E-mail: dieter.fauconnier@ugent.be

Contract/grant sponsor: Institute for the Promotion of Innovation through Science and Technology in Flanders (IWT-Vlaanderen)

*dynamic procedure*, in combination with an appropriate model for the truncation error, to obtain higher numerical accuracy [3]. We also showed that Richardson extrapolation can be seen as a simplified formulation of this procedure. In the present work, we investigate the role of the blending factor and the corresponding variation of the dynamic coefficient. We apply the procedure to the lid-driven cavity and, in contrast to the previous work, we use now pressure stabilization in the discretization and improved boundary conditions at the lid. Moreover, an eighth-order reference solution was created for more reliable error evaluation.

### 2. THE SAMPLING FORMALISM

We define the *sampling operator*  $\mathcal{S}^{\Delta_1}$ , which operates between the continuum space  $\Omega \subset \mathbb{R}^n$  and the discrete space  $\Omega^{\Delta_1}$  with number of grid points  $N_1$ , and spacing  $\Delta_1$ . This sampling operator  $\mathcal{S}^{\Delta_1}$  is idempotent and commutative with the product of the non-linear terms, but does not commute with spatial derivatives. We use notations  $\mathcal{S}^{\Delta_1} \circ u_i = \bar{u}_i$  and  $\mathcal{S}^{\Delta_1} \circ \partial = \delta$ . Applying  $\mathcal{S}^{\Delta_1}$  to the continuity equation and the momentum equations gives

$$\frac{\delta \bar{u}_i}{\delta x_i} = \Pi^{\Delta_1} \tag{1}$$

$$\frac{\partial \bar{u}_i}{\partial t} + \bar{u}_j \frac{\delta \bar{u}_i}{\delta x_j} = -\frac{\delta \bar{p}}{\delta x_i} + \nu \frac{\delta^2 \bar{u}_i}{\delta x_j^2} + \Sigma_i^{\Delta_1} \tag{2}$$

The truncation errors arise due to the non-commutativity of the operator  $\mathcal{S}^{\Delta_1}$  with the spatial derivatives, and have the basic form

$$\Pi^{\Delta_1} = \frac{\delta \bar{u}_i}{\delta x_i} - \overline{\frac{\partial u_i}{\partial x_i}} \tag{3}$$

$$\Sigma_i^{\Delta_1} = \bar{u}_j \left( \frac{\delta \bar{u}_i}{\delta x_j} - \overline{\frac{\partial u_i}{\partial x_j}} \right) + \left( \frac{\delta \bar{p}}{\delta x_i} - \overline{\frac{\partial p}{\partial x_i}} \right) - \nu \left( \frac{\delta^2 \bar{u}_i}{\delta x_j^2} - \overline{\frac{\partial^2 u_i}{\partial x_j^2}} \right) \tag{4}$$

### 3. THE GENERALIZED DYNAMIC PROCEDURE

Projection is done of the Navier–Stokes equations from a continuum domain  $\Omega$  to a corresponding discrete domain  $\Omega^{\Delta_1}$  and to  $\Omega^{\Delta_2}$  with the number of gridpoints  $N_2 < N_1$  ( $\Omega^{\Delta_2} \subset \Omega^{\Delta_1}$ ). This corresponds with the sampling operators  $\mathcal{S}^{\Delta_1}$  and  $\mathcal{S}^{\Delta_2}$  projecting, respectively,  $\Omega \rightarrow \Omega^{\Delta_1}$  and  $\Omega \rightarrow \Omega^{\Delta_2}$ .  $\mathcal{S}^{\Delta_2}$  also projects  $\Omega^{\Delta_1} \rightarrow \Omega^{\Delta_2}$ , since  $\mathcal{S}^{\Delta_2} \circ \mathcal{S}^{\Delta_1} = \mathcal{S}^{\Delta_2}$ . We introduce  $\mathcal{S}^{\Delta_2} \circ u_i = \tilde{u}_i = \tilde{\tilde{u}}_i$ . We keep the notation for the discrete derivative operator  $\mathcal{S}^{\Delta_2} \circ \partial = \delta$ . Applying the operator  $\mathcal{S}^{\Delta_1}$  on the continuous set of equations leads to

$$0 = \mathcal{C}^{\Delta_1}(\bar{u}_i) + \Pi^{\Delta_1} = -\frac{\delta \bar{u}_i}{\delta x_i} + \Pi^{\Delta_1} \tag{5}$$

$$\frac{\partial \bar{u}_i}{\partial t} = \mathcal{N}_i^{\Delta_1}(\bar{u}_i) + \Sigma_i^{\Delta_1} = -\bar{u}_j \frac{\delta \bar{u}_i}{\delta x_j} - \frac{\delta \bar{p}}{\delta x_i} + \nu \frac{\delta^2 \bar{u}_i}{\delta x_j^2} + \Sigma_i^{\Delta_1} \tag{6}$$

Here,  $\mathcal{C}^{\Delta_1}$  and  $\mathcal{N}_i^{\Delta_1}$  are called the continuity and Navier–Stokes operators, respectively. Applying  $\mathcal{S}^{\Delta_2}$  to the continuous set of equations gives

$$0 = \mathcal{C}^{\Delta_2}(\tilde{u}_i) + \Pi^{\Delta_2} = -\frac{\delta \tilde{u}_i}{\delta x_i} + \Pi^{\Delta_2} \tag{7}$$

$$\frac{\partial \tilde{u}_i}{\partial t} = \mathcal{N}_i^{\Delta_2}(\tilde{u}_i) + \Sigma_i^{\Delta_2} = -\tilde{u}_j \frac{\delta \tilde{u}_i}{\delta x_j} - \frac{\delta \tilde{p}}{\delta x_i} + \nu \frac{\delta^2 \tilde{u}_i}{\delta x_j^2} + \Sigma_i^{\Delta_2} \tag{8}$$

Ideally, the latter set should also be obtained by applying the sampling operator  $\mathcal{S}^{\Delta_2}$  to the first set of Equations (5)–(6) and because of  $\mathcal{S}^{\Delta_2} \circ \mathcal{S}^{\Delta_1} = \mathcal{S}^{\Delta_2}$ , the following relations are implied:

$$\mathcal{S}^{\Delta_2} \circ \mathcal{C}^{\Delta_1}(\bar{u}_i) - \mathcal{C}^{\Delta_2}(\tilde{u}_i) = \Pi^{\Delta_2} - \mathcal{S}^{\Delta_2} \circ \Pi^{\Delta_1} \tag{9}$$

$$\mathcal{S}^{\Delta_2} \circ \mathcal{N}_i^{\Delta_1}(\bar{u}_i) - \mathcal{N}_i^{\Delta_2}(\tilde{u}_i) = \Sigma_i^{\Delta_2} - \mathcal{S}^{\Delta_2} \circ \Sigma_i^{\Delta_1} \tag{10}$$

These explicitly express the commutation errors made by the projection  $\Omega^{\Delta_1} \rightarrow \Omega^{\Delta_2}$ . The expressions can be determined in terms of the resolved velocity  $\bar{u}_i$  since  $\mathcal{S}^{\Delta_2} \circ u_i = \tilde{u}_i = \bar{u}_i$ . Suppose models are adopted for the truncation errors  $\Pi^{\Delta_1}$  and  $\Sigma_i^{\Delta_1}$  consisting of a grid-independent scalar field denoted by  $C$ , and a grid-dependent model part denoted by  $m$ , such that  $\Pi^{\Delta_1} \approx C^\pi m^{\pi, \Delta_1}$  and  $\Sigma_i^{\Delta_1} \approx C_i^\sigma m_i^{\sigma, \Delta_1}$ . Analogously for the test level,  $\Delta_2$ .  $C^\pi$  and  $C_i^\sigma$  are fully determined by relations (9)–(10), which can be rewritten in every node as

$$\mathcal{L}^\pi = C^\pi \mathcal{M}^\pi, \quad \mathcal{L}_i^\sigma = C_i^\sigma \mathcal{M}_i^\sigma \tag{11}$$

To avoid possible singularities leading to instability of the method, we suggest to use a least-squares approximation to determine the grid-independent factors:

$$C = \frac{\langle \mathcal{L} \mathcal{M} \rangle}{\langle \mathcal{M} \mathcal{M} \rangle} \tag{12}$$

in which  $\langle \cdot \rangle$  denotes the average over the whole field.

#### 4. ILLUSTRATION FOR A FIRST-ORDER DERIVATIVE

In order to show the relationship of the dynamic procedure to Richardson extrapolation and to assess the spectral quality of the method, we proceed with the analysis of a single finite difference derivative instead of using the complete set of Navier–Stokes equations. Therefore, consider the Taylor series expansions of the  $n$ th discrete derivative  $\delta^n u / \delta x^n$  on two grids with spacings  $\Delta$  and  $2\Delta$ , for a  $k$ th-order central scheme,

$$\frac{\delta^n u}{\delta x^n}(x) = \left. \frac{\delta^n \bar{u}}{\delta x^n} \right|^\Delta + c_k \Delta^k \left. \frac{\delta^{k+n} \bar{u}}{\delta x^{k+n}} \right|^\Delta \tag{13}$$

$$\frac{\partial^n u}{\partial x^n}(x) = \left. \frac{\delta^n \tilde{u}}{\delta x^n} \right|^{2\Delta} + c_k (2\Delta)^k \left( f \left. \frac{\delta^{k+n} \tilde{u}}{\delta x^{k+n}} \right|^{2\Delta} + (1-f) \left. \frac{\delta^{k+n} \bar{u}}{\delta x^{k+n}} \right|^\Delta \right) \tag{14}$$

We assume that the leading order truncation term is an adequate model for the complete truncation error. A blending factor  $f$  is introduced into the coarse grid equation to provide a switch between the dynamic procedure ( $f = 1$ ) and Richardson extrapolation ( $f = 0$ ), and to investigate intermediate behaviour. Applying the generalized dynamic procedure is equivalent to extracting an expression for  $c_k$  from (13) and (14) and substituting it into (13). Using the relationship

$$\delta^n \tilde{u} / \delta x^n |^{2\Delta} - \delta^n \bar{u} / \delta x^n |^\Delta = c_k^* (1 - 2^k) \Delta^k \delta^{k+n} \bar{u} / \delta x^{k+n} |^\Delta \tag{15}$$

from Richardson extrapolation, in which  $c_k^* = -\frac{1}{6}$ , the resulting expression can be written as

$$\frac{\partial^n u}{\partial x^n}(x) = \left. \frac{\delta^n \bar{u}}{\delta x^n} \right|^\Delta + \frac{c_k^*}{1 - \frac{2^k f}{(1-2^k)} \left( \frac{\left. \frac{\delta^{k+n} \tilde{u}}{\delta x^{k+n}} \right|^{2\Delta} - \left. \frac{\delta^{k+n} \bar{u}}{\delta x^{k+n}} \right|^\Delta}{\left. \frac{\delta^{k+n} \bar{u}}{\delta x^{k+n}} \right|^\Delta} \right)} \Delta^k \left. \frac{\delta^{k+n} \bar{u}}{\delta x^{k+n}} \right|^\Delta \tag{16}$$

The Richardson extrapolation formula is obtained for a blending factor  $f = 0$  which is equivalent to imposing

$$\delta^{k+n} \tilde{u} / \delta x^{k+n} |^{2\Delta} \equiv \delta^{k+n} \bar{u} / \delta x^{k+n} |^\Delta \equiv \partial^{k+n} u / \partial x^{k+n} \tag{17}$$

leading to a  $(k + 2)$ th-order accurate central scheme for the  $n$ th derivative. It should be mentioned that  $c_k$  is obtained on the coarse grid and needs interpolation to the fine grid before substituting it into (13). Another possibility is evaluating  $c_k$  in every point on the fine grid; therefore, replacing  $\tilde{u}$  by  $\bar{u}$  in (14).

For further analysis of expression (16), a Fourier analysis for a *single wave* is performed for the second-order accurate gradient. Modified wavenumbers of the resulting expression are given in Figure 1 for several central schemes, and also for the dynamic expression (16) at values of  $f = 1, \frac{1}{2}, \frac{1}{3}, \frac{1}{4}, \frac{1}{5}, \frac{1}{10}$ . In case of  $f = 0$ , expression (16) collapses with the fourth-order scheme and is therefore not shown. Using a blending factor  $f = 1$  leads to a singularity at  $\kappa/\kappa_{\max} \approx 0.38$ , displaying a severe defect for the higher wavenumber range. However, decreasing this blending factor improves the spectral quality a lot. It can be noticed from the estimated accuracy plot, which compares the spectral behaviour of the procedure with the traditional standard schemes, that  $f = \frac{1}{5}$  optimizes the scheme for the lower wavenumber range, and should thus be ideal for the laminar flow calculations in this work. For the lower wavenumbers the accuracy is then slightly better than the sixth order, for the higher wavenumbers it is somewhat less. If the higher wavenumber range is more important, such as in some LES approaches or simulations with steep gradients, a choice

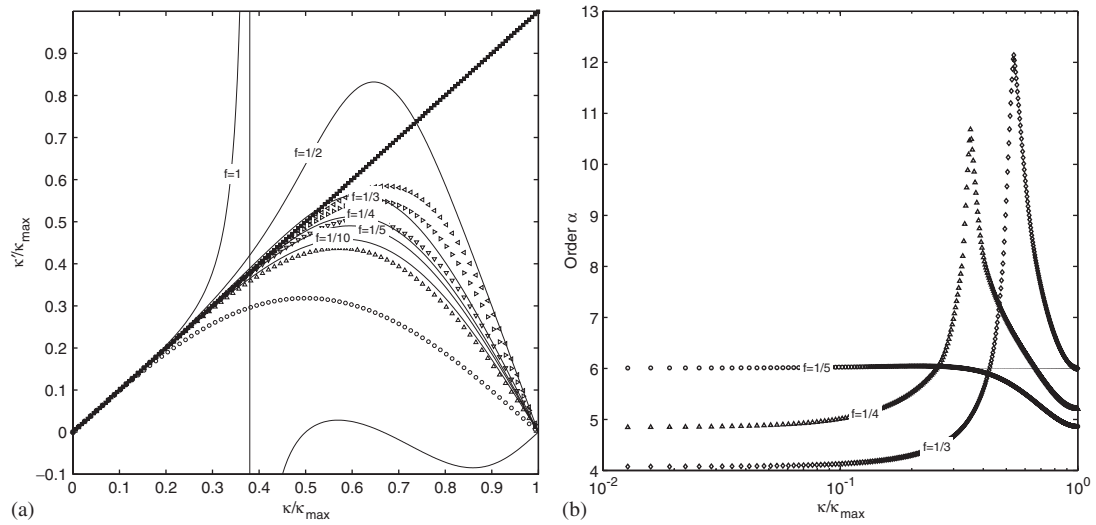


Figure 1. (a) Modified wavenumbers: (■) spectral; (○) second order; (△) fourth order; (▽) sixth order; (▷) eighth order; (◁) tenth order; (—) dynamic procedure and (b) estimated order of accuracy  $\alpha$ .

of  $f = \frac{1}{3}$  could be justified, such that the accuracy for the higher wavenumbers is more than sixth order, while maintaining the fourth order for lower ones.

### 5. MODELLING TRUNCATION ERRORS FOR NAVIER–STOKES EQUATIONS

Instead of evaluating a truncation correction and determining one dynamic constant for every distinct derivative in the Navier–Stokes equations, we try to increase the accuracy of the discretization by using a single model for all truncation errors in each equation and thus finding one dynamic constant for each equation. For a second-order central difference discretization scheme for first- and second-order partial derivatives, we suggest the following model. This *truncation error model* is obtained from the leading order truncation terms in the Taylor series expansion and the theoretical value of the factors  $C^\pi$  and  $C_i^\sigma$  is  $\frac{1}{6}$ :

$$\Pi^{\Delta_1} = C^\pi \Delta x_i^2 \frac{\delta^3 \bar{u}_i}{\delta x_i^3} \tag{18}$$

$$\Sigma_i^{\Delta_1} = C_i^\sigma \left( \bar{u}_j \Delta x_j^2 \frac{\delta^3 \bar{u}_i}{\delta x_j^3} + \Delta x_i^2 \frac{\delta^3 \bar{p}}{\delta x_i^3} - \frac{\nu}{2} \Delta x_j^2 \frac{\delta^4 \bar{u}_i}{\delta x_j^4} \right) \tag{19}$$

In the simulations  $C^\pi$  and  $C_i^\sigma$  are dynamically obtained using a least-squares method, as in (12). We also introduced a blending factor  $f$  straightforwardly, as done in Equations (13)–(14).

6. RESULTS

The test case is a steady laminar flow in a 2D lid-driven cavity at Reynolds number  $Re=400$ . In order to avoid the unphysical corner singularities for the pressure, the imposed velocity profile at the driven lid is chosen to be sinusoidal. A pseudo-compressible code is used with a third-order Runge–Kutta method for stepping in pseudo-time. The reference solution was generated on a  $120 \times 120$  uniform mesh with an eighth-order central scheme, and eighth-order excentric derivatives at the wall. We used a higher-order pressure stabilization  $\Gamma = \frac{1}{512} \Delta x_i^7 \partial^8 p / \partial x_i^8$  in the continuity equation in order to avoid interference with the accuracy as much as possible. All other simulations were done analogously on a  $60 \times 60$  mesh including the fourth- and sixth-order solutions used for comparison. For the continuity equation and the momentum equations, truncation error models (18) respectively (19) are used in combination with the dynamic procedure. The influence of the blending factor  $f$  is studied.

Results for the absolute errors of velocity,  $\varepsilon_u$  and  $\varepsilon_v$ , are shown in Figure 2 for the different simulations with different values of the blending factor. As expected from the wavenumber analysis, the dynamic procedure with the exact truncation model and  $f = \frac{1}{5}$  obtains an accuracy somewhat higher than the sixth-order solution. Results with the blending factors  $f = \frac{1}{4}$  and  $\frac{1}{3}$  give comparable error levels, although  $f = \frac{1}{4}$  tends to give slightly better results while  $f = \frac{1}{3}$  tends to do slightly worse. Further increase of the blending factor to  $f = \frac{1}{2}$  leads to an obvious deterioration, and for  $f = 1$ , the error levels exceed those of the fourth-order solution, illustrating the singularity in the modified wavenumber for this factor. Results for  $f = 0$  are not shown in Figure 2 as they

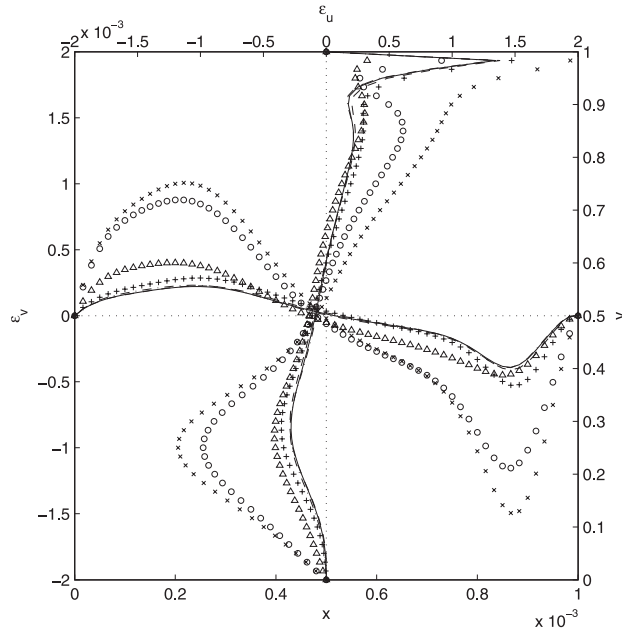


Figure 2. Error levels  $\varepsilon_u$  and  $\varepsilon_v$  in the cross-sections of the cavity  $y=L/2$  and  $x=L/2$ : ( $\Delta$ ) sixth-order; ( $o$ ) fourth-order; ( $\times$ )  $f=1$ ; ( $+$ )  $f=\frac{1}{2}$ ; ( $- -$ )  $f=\frac{1}{3}$ ; ( $—$ )  $f=\frac{1}{4}$ ; ( $- \cdot -$ )  $f=\frac{1}{5}$ .

Table I. Numerical values of the dynamically obtained constants.

Constant	$f=0$	$f=\frac{1}{5}$	$f=\frac{1}{4}$	$f=\frac{1}{3}$	$f=\frac{1}{2}$	$f=1$
$C^\pi$	0.1667	0.1694	0.1699	0.1705	0.1708	0.1652
$C_x^\sigma$	0.1667	0.1633	0.1622	0.1603	0.1559	0.1400
$C_y^\sigma$	0.1667	0.1753	0.1770	0.1792	0.1834	0.1791

collapse with the fourth-order solution. All these observations confirm the theoretical analysis of the presented procedure. The numerical values of the dynamic constants for each value of the blending factors are given in Table I.

## 7. CONCLUSION

The presented results demonstrate the ability of a dynamic procedure in combination with an appropriate truncation error model to obtain higher accuracy. It was shown that the truncation error model in combination with a dynamically obtained constant for each equation leads to an accuracy slightly better than that of a sixth-order scheme. An optimal value of the blending factor can be chosen according to the physics of the flow, optimizing the scheme for higher or lower wavenumber ranges. The present technique could certainly be a useful tool in multigrid algorithms providing higher accuracy at minimal extra cost. For single grid computations, the gain in accuracy is in competition with the additional cost of the procedure.

## REFERENCES

1. Winckelmans G, Bricteux L, Georges L, Daeninck G, Jeanmart H. The sampling-based dynamic procedure for LES: investigations using finite differences. In *Ercoftac Series—Direct and Large-Eddy Simulations*, Lamballais E, Friederich R, Geurts BJ, Métais O (eds), vol. 6, Poitiers, Ercoftac. Springer: Berlin, September 2005; 183–190.
2. Knaepen B, Debliquy O, Carati D. Large-eddy simulation without filter. *Journal of Computational Physics* 2005; **205**:98–107.
3. Fauconnier D, De Langhe C, Dick E. The dynamic procedure for accuracy improvement of numerical discretizations in fluid mechanics. *Journal of Computational Physics* 2007; **224**:1095–1123.